Treatment of Sickle Cell Anemia Mouse Model with iPS Cells Generated from Autologous Skin

Jacob Hanna, *et al.*

Science **318**, 1920 (2007);
DOI: 10.1126/science.1152092

Science (print ISSN 0036-8075; online ISSN 1095-9203) is published weekly, except the last week in December, by the American Association for the Advancement of Science, 1200 New York Avenue NW, Washington, DC 20005.

involves the destruction of human preimplantation embryos, and iPS cells remove this concern. However, further work is needed to determine whether human iPS cells differ in clinically important ways from ES cells.

References and Notes

1. I. Wilmut, A. E. Schnieke, J. McWhir, A. J. Kind, K. H. Campbell, *Nature* **385**, 810 (1997).
2. N. Maherali *et al*., *Cell Stem Cell* **1**, 55 (2007).
3. K. Okita, T. Ichisaka, S. Yamanaka, *Nature* **448**, 313 (2007).
4. K. Takahashi, S. Yamanaka, *Cell* **126**, 663 (2006).
5. M. Wernig *et al*., *Nature* **448**, 318 (2007).
6. T. Sumi, N. Tsuneyoshi, N. Nakatsuji, H. Suemori, *Oncogene* **26**, 5564 (2007).
7. J. Yu, M. A. Vodyanik, P. He, I. I. Slukvin, J. A. Thomson, *Stem Cells* **24**, 168 (2006).
8. T. P. Zwaka, J. A. Thomson, *Nat. Biotechnol.* **21**, 319 (2003).
9. M. A. Vodyanik, J. A. Bork, J. A. Thomson, I. I. Slukvin, *Blood* **105**, 617 (2005).
10. Materials and methods are available as supporting material on *Science* Online.
11. J. Silva, I. Chambers, S. Pollard, A. Smith, *Nature* **441**, 997 (2006).
12. H. Darr, Y. Mayshar, N. Benvenisty, *Development* **133**, 1193 (2006).
13. E. Birney *et al*., *Nature* **447**, 799 (2007).
14. J. A. Thomson *et al*., *Science* **282**, 1145 (1998).
15. A. Meissner, M. Wernig, R. Jaenisch, *Nat. Biotechnol.* **25**, 1177 (2007).

16. We thank the Charlotte Geyer Foundation for their support. Other funding included NIH grants P51 RR000167 and P20 GM069981. We thank K. J. Heidarsdottir, B. K. Gisladottir, M. Probasco, and C. Glennon for technical assistance, and D. J. Faupel for critical reading of the manuscript. The authors declare competing financial interests. J.A.T. owns stock, serves on the Board of Directors, and serves as Chief Scientific Officer of Cellular Dynamics International and Stem Cell Products. J.A.T. also serves as Scientific Director of the WiCell Research Institute. Microarray data have been deposited in the Gene Expression Omnibus (GEO) database (accession number GSE9164).

Supporting Online Material

www.sciencemag.org/cgi/content/full/1151526/DC1
Materials and Methods
Figs. S1 to S10
Tables S1 to S7
References

9 October 2007; accepted 14 November 2007
Published online 20 November 2007;
10.1126/science.1151526
Include this information when citing this paper.

Treatment of Sickle Cell Anemia Mouse Model with iPS Cells Generated from Autologous Skin

Jacob Hanna,[1] Marius Wernig,[1] Styliani Markoulaki,[1] Chiao-Wang Sun,[2] Alexander Meissner,[1] John P. Cassady,[1,3] Caroline Beard,[1] Tobias Brambrink,[1] Li-Chen Wu,[2] Tim M. Townes,[2]* Rudolf Jaenisch[1,3]*

It has recently been demonstrated that mouse and human fibroblasts can be reprogrammed into an embryonic stem cell–like state by introducing combinations of four transcription factors. However, the therapeutic potential of such induced pluripotent stem (iPS) cells remained undefined. By using a humanized sickle cell anemia mouse model, we show that mice can be rescued after transplantation with hematopoietic progenitors obtained in vitro from autologous iPS cells. This was achieved after correction of the human sickle hemoglobin allele by gene-specific targeting. Our results provide proof of principle for using transcription factor–induced reprogramming combined with gene and cell therapy for disease treatment in mice. The problems associated with using retroviruses and oncogenes for reprogramming need to be resolved before iPS cells can be considered for human therapy.

A major goal of human therapy is to develop methods that allow treatment of patients afflicted with genetic and degenerative disorders with a ready supply of defined transplantable cells. This has raised great interest in embryonic stem (ES) cells, which have the potential to generate all cell types in culture (*1*). ES cell–based therapy, however, would be complicated by immune rejection due to immunological incompatibility between patient and donor cells. As a result, the concept of deriving genetically identical "customized" ES-like cells by somatic cell nuclear transfer (SCNT) using a donor cell from the patient was developed (*2*). This strategy was expected to eliminate the requirement for immune suppression (*3*), but technical and ethical complexities of SCNT impede the practical realization of "therapeutic cloning" (*4*).

In a recent series of studies, mouse and human fibroblasts were reprogrammed in vitro into pluripotent stem cell–like cells (termed "induced pluripotent stem cells," or iPS) through retroviral transduction of combinations of transcription factors (*5*–*9*). This was achieved by selection for reprogrammed cells by reactivation of marked endogenous pluripotency genes Oct4 or Nanog or by subcloning of colonies based on morphological criteria (*5*–*11*). iPS cells derived from mouse and human fibroblasts are highly similar to ES cells by genetic, epigenetic, and developmental criteria. However, it remained to be determined whether mouse iPS cells obtained from adult fibroblasts can serve to restore physiological function of diseased tissues in vivo.

To gain insights into the therapeutic applicability of mouse iPS cells, we evaluated whether hematopoietic progenitors (HPs) could be derived from iPS cells in vitro for subsequent engrafting into adult recipients (*12*). Tail-tip fibroblasts were isolated from a 2-week-old Oct4-Neomycin knock-in mouse (*8*) and a 3-month-old genetically unmodified mouse. Cells were transduced with retroviruses encoding for Oct4, Sox2, Klf4, and c-Myc transcription factors (*13*). Neomycin was added 9 days after infection to fibroblasts derived from Oct4-neo mouse to select for cells that reactivated the endogenous Oct4 gene, a master regulator of pluripotency, and neomycin-resistant colonies were picked on day 20. Transduced fibroblasts from genetically unmodified mice gave rise to colonies that were picked based on morphological criteria (*10*, *11*). Ten out of 12 picked clones eventually generated cell lines with ES-like morphology that expressed ES cell markers AP, SSEA1, and Nanog. Lines designated as ITT026 and ITT4 iPS were randomly chosen from Oct4-Neo and unmodified donor cells, respectively, for further analysis (fig. S1).

Ectopic expression of homeodomain protein HoxB4 in differentiating ES cells has been shown to confer engraftment potential on in vitro–derived hematopoietic cells from ES cells grown in hematopoietic cytokines on the OP9 bone marrow stroma cell line, which has been shown to support hematopoietic differentiation (*12*, *14*). Dissociated embryoid body (EB) differentiated cells generated from V6.5 ES cells and fibroblast-derived ITTO26 and ITT4 iPS cells were infected with Moloney virus encoding green fluorescent protein (GFP)–tagged HoxB4 protein (*12*). Cells expressing CD41 and c-kit antigens (markers of early HPs), as well as markers for myeloid and erythroid differentiation, were detected at similar levels on cells differentiated from the ES and iPS lines (Fig. 1A and fig. S2). Moreover, methylcellulose colony formation assays showed that all samples formed a variety of immature and mature myeloid colonies at comparable frequencies (Fig. 1B and fig. S3). We next transplanted these in vitro–generated HPs into irradiated genetically identical adult C57black6/129Sv F1 recipient mice. HPs from both ES and iPS cells conveyed multilineage reconstitution of recipient mice, as determined by GFP content in peripheral blood for up to 20 weeks, and rescued the mice from lethal irradiation (Fig. 1C). Fluorescence-activated cell sorting (FACS) analysis showed predominant myeloid lineage formation from the transplanted progenitors (fig. S4), consistent with previous studies (*12*, *14*, *15*).

These experiments prompted us to evaluate the therapeutic potential of iPS cells derived from adult fibroblasts of mice afflicted with a genetic disorder of the hematopoietic system. The general therapeutic strategy applied involved (i) reprogramming of mutant donor fibroblasts into iPS cells, (ii) repair of the genetic defect through homologous recom-

[1]The Whitehead Institute for Biomedical Research, Cambridge, MA 02142, USA. [2]Department of Biochemistry and Molecular Genetics, University of Alabama at Birmingham, Schools of Medicine and Dentistry, Birmingham, AL 35294, USA. [3]Massachusetts Institute of Technology, Department of Biology, Cambridge, MA 02142, USA.

*To whom correspondence should be addressed. E-mail: Jaenisch@wi.mit.edu (R.J.); ttownes@uab.edu (T.M.T.)

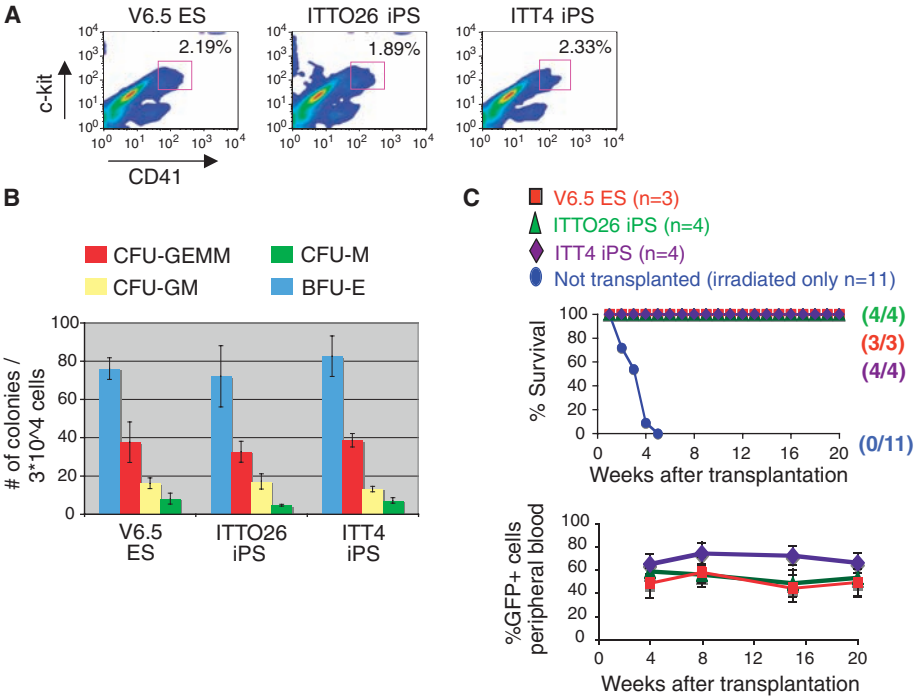

Fig. 1. Hematopoietic reconstitution by iPS cell in vitro–derived HPs. (**A**) FACS analysis of CD41 and c-kit on ES and iPS differentiated cells grown on OP-9 stroma for 6 days. (**B**) Quantitative comparison of various types of hematopoietic colonies obtained in methylcellulose cultures from iPS- and ES-derived differentiated cells grown with myeloid cytokines for 6 days. CFU, colony forming unit; GEMM, granulocyte, erythroid, macrophage, megakaryocyte multilineage; BFU-E, blood forming unit–erythroid; M, monocyte; GM, granulocyte macrophage. One out of two independent experiments is shown. (**C**) Survival curve and the percentage of GFP-positive ES- and IPS-derived HPs in the peripheral blood of transplanted or nontransplanted recipients at indicated time points after transplantation.

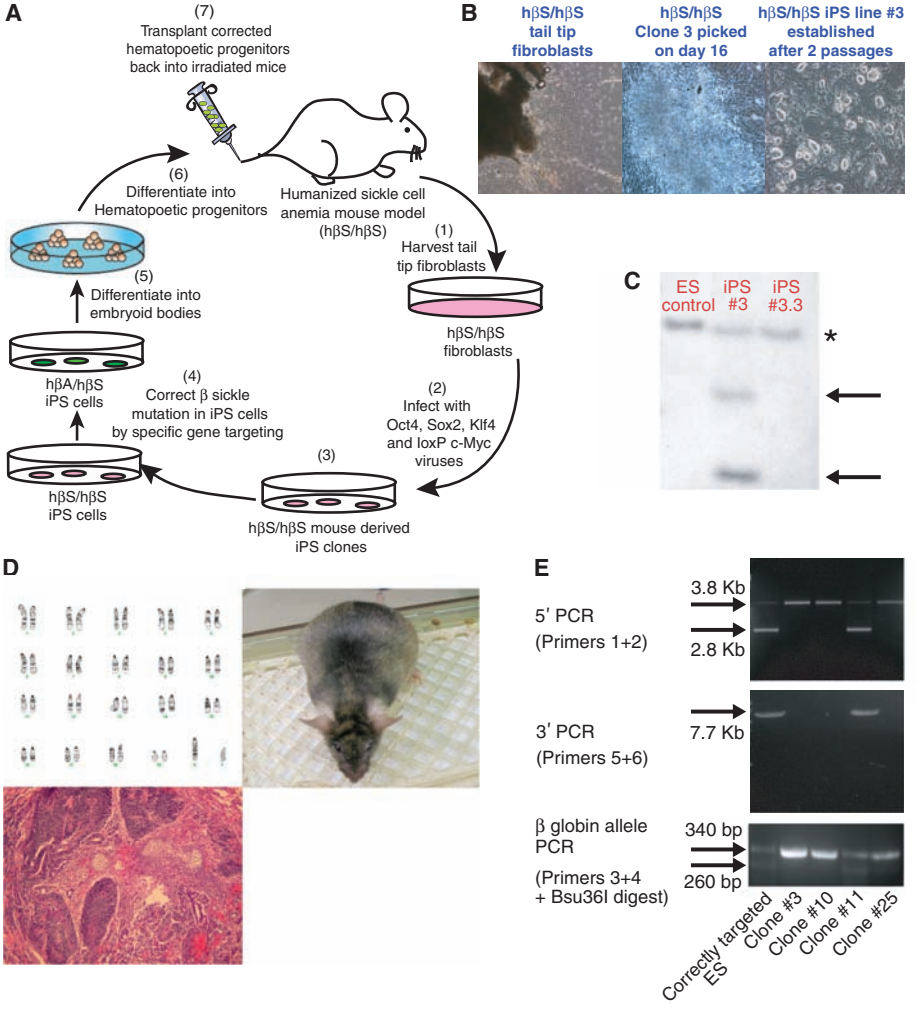

Fig. 2. Derivation of autologous iPS cells from $h\beta^S/h\beta^S$ mice and correction of the sickle allele by gene targeting. (**A**) Scheme for in vitro reprogramming of skin fibroblasts with defined transcription factors combined with gene and cell therapy to correct sickle cell anemia in mice. (**B**) Representative images of various steps of deriving $h\beta^S/h\beta^S$ iPS line #3. (**C**) Southern blot for c-Myc viral integrations in (i) ES cells, (ii) $h\beta^S/h\beta^S$ iPS line #3 and (iii) its derived subclone $h\beta^S/h\beta^S$ iPS #3.3 obtained after infection with adeno-Cre virus and deletion of the viral c-Myc copies. * indicates endogenous c-Myc band. Arrows point to transgenic copies of c-Myc. (**D**) $h\beta^S/h\beta^S$ iPS#3.3 displayed normal karyotype 40XY (upper left), was able to generate viable chimeras (upper right), and formed teratomas (bottom). (**E**) Replacement of the $h\beta^S$ gene with a $h\beta^A$ globin gene in sickle iPS cell line #3.3. Homologous recombinants were identified by PCR to identify correct 5′ and 3′ end replacement. PCR with primers 3 and 4 followed by Bsu36I digestion was used to distinguish $h\beta^S$ and $h\beta^A$ alleles. Correctly targeted clone #11 displayed identical pattern to that previously obtained for correctly targeted ES cell clone.

bination, (iii) in vitro differentiation of repaired iPS cells into HPs, and (iv) transplanting these cells into affected donor mice after irradiation (Fig. 2A).

We chose a humanized knock-in mouse model of sickle cell anemia in which the mouse α-globin genes were replaced with human α-globin genes, and the mouse β-globin genes were replaced with human Aγ and β^S (sickle) globin genes (*16*). Homozygous mice for the human β^S allele remain viable for up to 18 months but develop typical disease symptoms such as severe anemia due to erythrocyte sickling, splenic infarcts, urine concentration defects, and overall poor health (*16*). To conduct this "proof of principle" experiment, we established tail-tip–derived fibroblast cultures from an adult 12-week-old $h\beta^S/h\beta^S$ male and infected the cells with retroviruses encoding for Oct4, Sox2, and Klf4 factors and a lentivirus encoding a 2-lox c-Myc cDNA (Fig. 2B). Twenty-four clones were isolated on day 16 after infection, expanded on feeder cells, and iPS line #3 was randomly selected for further experiments. To reduce the potential risk of tumor formation due to c-Myc transgene expression (*13*), iPS cells were infected with an adenovirus encoding Cre-recombinase to delete the lentivirus-transduced c-Myc copies. One out of 10 iPS subclones (iPS #3.3) had deleted both transduced copies of c-Myc and was used for further experimentation (Fig. 2C). This subcloned cell line stained positive for pluripotency markers, had a normal karyotype, and generated teratomas and chimeras (Fig. 2D, fig. S5, and table S1).

To achieve specific gene correction of the $h\beta^S$ alleles, iPS #3.3 cells were electroporated with a targeting construct containing the human β^A wild-type globin gene (fig. S6) (*16*). Hygromycin- and gancyclovir-resistant cells were screened for correct gene targeting, and one of 72 drug resistant iPS colonies was identified as correctly targeted (clone #11) (Fig. 2E). This result shows that iPS cells can be targeted by homologous recombination at comparable efficiency to that of ES cells (*16*).

We next evaluated whether HPs derived in vitro from corrected iPS cells were able to reconstitute the hematopoietic system of sickle mice and correct their disease phenotype. Three $h\beta^S/h\beta^S$ male mice were irradiated and transplanted with corrected iPS# 3.3.11–derived HPs. All three mice demonstrated stable engraftment based on the presence of GFP+ cells in the peripheral blood for up to 12 weeks after transplantation (Fig. 3A and fig. S7). Further evidence for engraftment was shown by polymerase chain reaction (PCR) analysis of the genomic DNA from peripheral blood of treated and untreated $h\beta^S/h\beta^S$ mice using primers that amplify both $h\beta^S$ and $h\beta^A$ alleles producing 340-bp amplicons. Digestion of the amplicons with Bsu36I restriction enzyme, which cleaves the $h\beta^A$ but not the $h\beta^S$ allele (*16*), showed that DNA from peripheral blood of treated mice carried the specific bands

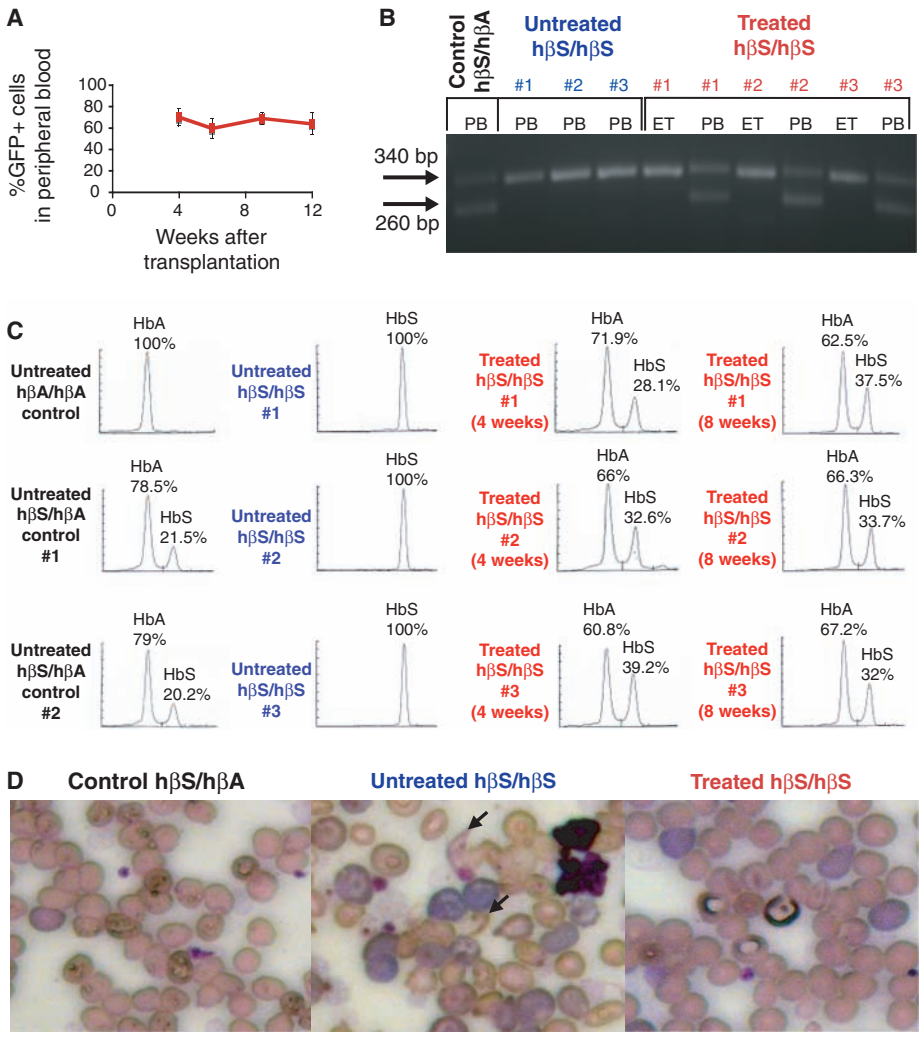

Fig. 3. Correction of sickle cell anemia phenotype by autologous genetically corrected iPS-derived HPs. (**A**) Average GFP+ content in transplanted $h\beta^S/h\beta^S$ recipients at indicated time points after transplantation (n = 3). (**B**) Specific detection of cells carrying $h\beta^A$ allele in blood of treated $h\beta^S/h\beta^S$ recipients by PCR in whole peripheral blood (PB) DNA followed by Bsu36I digestion. Ear-tip (ET) fibroblasts from treated $h\beta^S/h\beta^S$ mice were obtained and grown in culture 3 weeks after transplant. (**C**) Electrophoresis detection of human β globin protein in peripheral blood of $h\beta^A/h\beta^A$, $h\beta^A/h\beta^S$, untreated $h\beta^S/h\beta^S$, and treated $h\beta^S/h\beta^S$ mice 4 and 8 weeks after transplant. (**D**) Representative Wright-Giemsa stained blood smears of $h\beta^A/h\beta^S$, treated (8 weeks after transplant), and untreated $h\beta^S/h\beta^S$ mice. Arrows indicate representative sickled deformed erythrocytes.

Table 1. Restitution of disease parameters by corrected IPS-derived HPs. Hematological parameters presented were obtained 8 and 12 weeks after corrective bone marrow transplantation. Parameters for untreated $h\beta^S/h\beta^S$ and $h\beta^A/h\beta^S$ mice are used as controls. Values represent the mean ± SD. Statistical significance was determined for $h\beta^S/h\beta^S$ treated mice compared with untreated $h\beta^S/h\beta^S$ controls; P values were calculated using Student's t test; n = 3 each group. *, $P < 0.01$; **, $P < 0.05$. Weight values were taken from aged matched mouse groups (17 weeks of age). RBC indicates red blood cell count; Hb, hemoglobin; PCV, packed cell volume or hematocrit; RDW, red cell distribution width; MCV, mean corpuscular volume; fl, femoliter.

Mouse group (n = 3)	Hb (g/dl)	RBC (×10^6/μl)	PCV (%)	Reticulocytes (%)	RDW (%)	MCV (fl)	Urine concentration (mOsm)	Breaths (per min)	Weight (g)
$h\beta^A/h\beta^S$ control	16.1±1.3	14.7±1.7	55.8±3.1	4.53±0.7	21.9±0.9	39.5±1.1	2378±135	49.6±4.3	28.9±1.2
$h\beta^S/h\beta^S$ untreated	8.86±1.5	6.75±0.2	32.1±5.4	26.8±3.1	29.5±1.58	47.5±1.2	885±149	78.6±9.1	18.9±0.7
$h\beta^S/h\beta^S$ treated (8 weeks)	14.3±0.9*	11.8±0.7*	50.8±6.2*	9.9±2.8*	22.5±1.5*	41.4±3.0**	1827±291*	55.2±6.0*	22.8±1.4**
$h\beta^S/h\beta^S$ treated (12 weeks)	13.63±0.3*	12.62±0.6*	50.0±2.0*	10.0±1.1*	21.5±0.9*	39.7±0.7*	1754±226*	59.2±5.2**	24.1±1.2*

characteristic of the $h\beta^A$ and the $h\beta^S$ alleles (Fig. 3B). DNA samples from control $h\beta^S/h\beta^S$ mice, as well as from ear fibroblasts of treated $h\beta^S/h\beta^S$ mice, did not display any bands corresponding to the $h\beta^A$ allele (Fig. 3B).

Functional correction of the sickle cell defect was evaluated by electrophoresis for human β globin proteins A and S (HbA and HbS) in blood of untreated and treated $h\beta^S/h\beta^S$ mice. Stable and significant detection of HbA protein (mean of 65% versus 0% out of total β globin protein in untreated $h\beta^S/h\beta^S$ mice, $P < 0.01$) (fig. S8) and pronounced reduction in HbS protein 4 and 8 weeks after transplantation were seen in the blood of treated mice (Fig. 3C). Treated $h\beta^S/h\beta^S$ mice had higher levels of HbS than control heterozygous $h\beta^A/h\beta^S$ animals, most likely because only ~70% of the peripheral blood cells were derived from the iPS cells (Fig. 3A).

Morphological analysis of red blood cells (RBCs) in blood smears of untreated $h\beta^S/h\beta^S$ mice demonstrated an abundance of rigid elongated cells, consistent with sickle cell disease, and severe reticulocytosis (Fig. 3D) (*13*). In contrast, blood smears of the treated animals had a lower degree of polychromasia, which is consistent with decreased reticulocyte levels. Also, anisocytosis and poikolocytosis were decreased in treated animals (Fig. 3D). Blood count follow-up tests were performed up to 12 weeks after transplantation. Compared with untreated $h\beta^S/h\beta^S$ mice, the treated animals had marked increases in RBC counts, hemoglobin, and packed cell volume levels (Table 1). Furthermore, $h\beta^S/h\beta^S$ mice showed normalized mean corpuscular volume (MCV) and red cell distribution width (RDW) index values, which are objective parameters for anisocytosis and poikolocytosis (Table 1 and Fig. 3D). An important indicator of sickle cell disease activity and severity is the elevated level of reticulocytes in peripheral blood, which are immature RBCs (*17*), reflecting increased production of RBCs to overcome their chronic loss. Reticulocyte count was dramatically reduced in blood of recipient sickle mice after corrective bone marrow transplantation (Table 1).

Finally, we examined whether the urine concentration defect, which results from RBC sickling in renal tubules and consequent reduction in renal medullary blood flow (*18*, *19*), and the general deteriorated systemic condition reflected by lower body weight and increased breathing (*16*), had been improved. All three pathological features were ameliorated in treated $h\beta^S/h\beta^S$ mice (Table 1). In summary, our results indicate that all hematological and systemic parameters of sickle cell anemia improved substantially and were comparable to those in control mice (Fig. 3 and Table 1). Although none of the mice transplanted with iPS-derived cells showed any evidence of tumor formation, the possibility remains that malignancy may develop at later time points as a result of transgenes encoding oncogenic proteins (*13*).

The ethical debate over "therapeutic cloning," as well as the technical difficulty and inefficiency of the process (*20*), has spurred the quest to achieve reprogramming of somatic cells by defined factors (*5*–*9*, *13*). The recent strategy of deriving iPS cells from genetically unmodified donor cells based on morphological criteria (*10*, *11*), as devised in this study to derive iPS cells from mice with sickle cell anemia, has simplified their potential use for therapeutic application or for studying diseases. The correction of sickle cell anemia described in our experiments indicates that harnessing autologous iPS-derived cells for therapeutic purposes recapitulates several of the promises offered previously by SCNT: (i) no requirement for administration of immunosuppressive drugs to prevent rejection of the unmatched transplanted cells, (ii) the opportunity to repair genetic defects by homologous recombination, and (iii) the opportunity to repeatedly differentiate iPS cells into the desired cell type for continued therapy.

Even though reprogramming of human somatic cells into iPS cells has now been achieved (*6*, *9*), future therapeutic application of iPS cells in humans requires overcoming several obstacles: (i) bypassing the use of harmful oncogenes as part of the reprogramming factors (*13*), (ii) avoiding the use for gene delivery of retroviral vectors that carry the risk of insertional mutagenesis, and (iii) developing robust and reliable differentiation protocols for human iPS cells. Current advances in molecular reprogramming set the stage for devising alternative strategies, such as transient gene expression vectors, engineered membrane-permeable transcription factor proteins, or small molecules that can replace potentially hazardous factors and lessen the risk of cancer associated with the current reprogramming approach.

References and Notes

1. P. H. Lerou, G. Q. Daley, *Blood Rev.* **19**, 321 (2005).
2. R. Jaenisch, *N. Engl. J. Med.* **351**, 2787 (2004).
3. W. M. Rideout 3rd, K. Hochedlinger, M. Kyba, G. Q. Daley, R. Jaenisch, *Cell* **109**, 17 (2002).
4. I. L. Weissman, *Nature* **439**, 145 (2006).
5. N. Maherali *et al.*, *Cell Stem Cell* **1**, 55 (2007).
6. K. Takahashi *et al.*, *Cell* **131**, 861 (2007).
7. K. Takahashi, S. Yamanaka, *Cell* **126**, 663 (2006).
8. M. Wernig *et al.*, *Nature* **448**, 318 (2007).
9. J. Yu *et al.*, *Science*. Published online 20 November 2007; 10.1126/science.1151526.
10. R. Blelloch *et al.*, *Cell Stem Cell* **1**, 245 (2007).
11. A. Meissner, M. Wernig, R. Jaenisch, *Nat. Biotechnol.* **25**, 1177 (2007).
12. M. Kyba, R. C. Perlingeiro, G. Q. Daley, *Cell* **109**, 29 (2002).
13. K. Okita, T. Ichisaka, S. Yamanaka, *Nature* **448**, 313 (2007).
14. S. Eckardt *et al.*, *Genes Dev.* **21**, 409 (2007).
15. Y. Wang, F. Yates, O. Naveiras, P. Ernst, G. Q. Daley, *Proc. Natl. Acad. Sci. U.S.A.* **102**, 19081 (2005).
16. L. C. Wu *et al.*, *Blood* **108**, 1183 (2006).
17. H. F. Bunn, *N. Engl. J. Med.* **337**, 762 (1997).
18. R. Pawliuk *et al.*, *Science* **294**, 2368 (2001).
19. T. M. Ryan, D. J. Ciavatta, T. M. Townes, *Science* **278**, 873 (1997).
20. K. Hochedlinger, R. Jaenisch, *Nature* **441**, 1061 (2006).

21. We would like to thank J. Goldberg, F. Camargo, K. Pawlik, J. Dausmann, K. Velletrie, Y. Lai, and members of the Jaenisch and Townes laboratories for excellent assistance; and K. Humphries and G. Sauvageau for HoxB4 viral constructs. R.J. is supported by NIH grants 5-RO1-HDO45022, 5-R37-CA084198, and 5-RO1-CA087869, and T.M.T. by NIH grant 2-R01-HL057619. J.P.C. is a Howard Hughes Medical Institute Gilliam Fellow. J.H. is a Novartis Fellow of the Helen Hay Whitney Foundation. The authors declare no conflict of interest.

Supporting Online Material

www.sciencemag.org/cgi/content/full/1152092/DC1
Materials and Methods
Figs. S1 to S8
Table S1
References

23 October 2007; accepted 26 November 2007
Published online 6 December 2007;
10.1126/science.1152092
Include this information when citing this paper.

Structure of $G\alpha_q$-p63RhoGEF-RhoA Complex Reveals a Pathway for the Activation of RhoA by GPCRs

Susanne Lutz,[1]* Aruna Shankaranarayanan,[2,3]* Cassandra Coco,[2] Marc Ridilla,[2]† Mark R. Nance,[2] Christiane Vettel,[1] Doris Baltus,[1] Chris R. Evelyn,[4] Richard R. Neubig,[4] Thomas Wieland,[1]‡ John J. G. Tesmer[2,4]‡

The guanine nucleotide exchange factor p63RhoGEF is an effector of the heterotrimeric guanine nucleotide–binding protein (G protein) $G\alpha_q$ and thereby links $G\alpha_q$-coupled receptors (GPCRs) to the activation of the small-molecular-weight G protein RhoA. We determined the crystal structure of the $G\alpha_q$-p63RhoGEF-RhoA complex, detailing the interactions of $G\alpha_q$ with the Dbl and pleckstrin homology (DH and PH) domains of p63RhoGEF. These interactions involve the effector-binding site and the C-terminal region of $G\alpha_q$ and appear to relieve autoinhibition of the catalytic DH domain by the PH domain. Trio, Duet, and p63RhoGEF are shown to constitute a family of $G\alpha_q$ effectors that appear to activate RhoA both in vitro and in intact cells. We propose that this structure represents the crux of an ancient signal transduction pathway that is expected to be important in an array of physiological processes.

Rho guanine nucleotide triphosphatases (GTPases) are peripheral membrane proteins that regulate essential cellular processes, including cell migration, proliferation, and contraction. RhoA, Rac1, and Cdc42 are the best-characterized members of this family, and they control the dynamics of the actin cytoskeleton and also stimulate gene transcription through several transcription factors, such as the serum response factor (SRF) or nuclear factor κB (*1*, *2*). All Rho GTPases cycle between an inactive guanosine diphosphate (GDP)–bound and an active guanosine